EurJIC
European Journal of Inorganic Chemistry

Research Article
doi.org/10.1002/ejic.202200772

Chemistry Europe
European Chemical Societies Publishing

www.eurjic.org

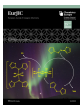

Ruthenium-Assisted Tellurium Abstraction in Bis(thiophen-2-yl) Ditelluride

Marjaana Taimisto,[a] Merja J. Poropudas,[a] J. Mikko Rautiainen,[b] Raija Oilunkaniemi,*[a] and Risto S. Laitinen*[a]

Dedicated to Prof. Dr. Wolfgang Weigand on the occasion of his 65th birthday.

The reaction of $[RuCl_2(CO)_3]_2$ and Te_2Tpn_2 (Tpn = thiophen-2-yl, C_4H_3S) in the absence of light resulted in the formation of *cct*-$[RuCl_2(CO)_2(TeTpn_2)_2]$ (**1**) [*cis*(Cl)-*cis*(CO)-*trans*($TeTpn_2$)] and $TeTpn_2$ (**2**) together with the precipitation of tellurium. The complex **1** and the monotelluride **2** were characterized by NMR spectroscopy and single-crystal X-ray diffraction. The decomposition of Te_2Tpn_2 to $TeTpn_2$ has been monitored by ^{125}Te NMR spectroscopy and seemed to be faster than the ligand substitution in $[RuCl_2(CO)_3]_2$ by $TeTpn_2$. A catalytic cycle is proposed for the decomposition of Te_2Tpn_2 to $TeTpn_2$ based on the PBE0-D3/def2-TZVP calculations.

Introduction

The telluroether complexes of ruthenium were reported already in the 1970s (for early literature, see reviews in refs.[1–3]), but it is only during the last three decades, that the structural chemistry of these complexes has attracted more research attention (see some recent reviews in Refs. [4-8]). Hieber and John[9,10] suggested that the reaction between diorganyl telluride TeR_2 (R = C_6H_5, C_4H_9) and $RuCl_3{\cdot}nH_2O$ or $[Ru(CO)_2X_2]_n$ (X = Br, I) affords mononuclear ruthenium(II) complexes $[RuX_2(CO)_n(TeR_2)_{4-n}]$ (n = 1, 2) and assessed their isomerism spectroscopically. The crystal structure determination of $[RuCl_2(CO)_2(TePh_2)_2]{\cdot}{}^1/_2\ C_6H_6$[11] verified their suggestion of the *cis*(CO)-*cis*(Cl)-*trans*(TeR_2) conformation (*cct*). The same isomer has been established for those members of $[RuCl_2(CO)_2(ERR')_2]$ (E = S, Se, Te; R, R' = Me, Ph), for which the crystal structure information is available,[8,11,12] as well as for the related $[RuCl_2(CO)_2\{Te(CH_2SiMe_3)_2\}_2]$.[13]

In this contribution we have explored the reaction of $[RuCl_2(CO)_3]_2$ with Te_2Tpn_2 (Tpn = thiophen-2-yl, C_4H_3S) with the objective to establish, how the organic ditelluride coordinates to the ruthenium center in $[RuCl_2(CO)_3]_2$. It turned out, however, that Te_2Tpn_2 decomposed to form $TeTpn_2$, and the end-product was *cct*-$[RuCl_2(CO)_2(TeTpn_2)_2]$ (**1**). Bis(thiophen-2-yl) telluride $TeTpn_2$ (**2**) could also be isolated from the reaction mixture together with elemental tellurium. The two formal reactions representing the total process are shown in Scheme 1. We were interested about the possible bifunctionality of $[RuCl_2(CO)_2]$ as a catalyst to the decomposition of Te_2Tpn_2 and as a reagent towards the ligand substitution by $TeTpn_2$. We have consequently explored the reaction pathway of the decomposition of Te_2Tpn_2 leading to the formation of **1**.

Results and Discussion

General

The reaction between $[RuCl_2(CO)_3]_2$ and Te_2Tpn_2 in the absence of light interestingly afforded $[RuCl_2(CO)_2(TeTpn_2)_2]$ (**1**) together with elemental tellurium, which precipitated during the reaction. This formally indicates the decomposition of the ditelluride to $TeTpn_2$ and Te(s) and the ligand substitution reactions by $TeTpn_2$ involving both ruthenium centers of $[RuCl_2(CO)_3]_2$ (see Scheme 1). The latter reaction is analogous to those involving $[RuCl_2(CO)_3]_2$ and ERR' (E = S, Se, Te; R, R' = Me, Ph), which have been discussed previously.[8–12]

The complex **1** was obtained as orange crystals. The molecular structure was verified as *cct*-$[RuCl_2(CO)_2(TeTpn_2)_2]$ by the single-crystal X-ray structure determination (see below). When the isolated crystals were dissolved in $CDCl_3$, only one ^{125}Te NMR resonance at 616 ppm was observed. This ^{125}Te chemical shift lies in the same region as that of *cct*-$[RuCl_2(CO)_2(TePh_2)_2]$ at 704 ppm[11] verifying the formation of compound **1** in the reaction.

In addition to using the formal stoichiometric ratio of 1 : 4 of $[RuCl_2(CO)_3]_2$ and Te_2Tpn_2 (see Scheme 1), the reaction was also carried out involving initial excess of $[RuCl_2(CO)_3]_2$ (molar ratio of the reactants 1 : 1), as well as using initial excess of Te_2Tpn_2

[a] M. Taimisto, Dr. M. J. Poropudas, Dr. R. Oilunkaniemi, Prof. R. S. Laitinen
Laboratory of Inorganic Chemistry
Environmental and Chemical Engineering
University of Oulu
P.O. Box 3000, 90014 Oulu (Finland)
E-mail: raija.oilunkaniemi@oulu.fi
risto.laitinen@oulu.fi
[b] Dr. J. M. Rautiainen
Department of Chemistry
Nanoscience Center
University of Jyväskylä
P.O. Box 35, 40014 Jyväskylä (Finland)

Supporting information for this article is available on the WWW under https://doi.org/10.1002/ejic.202200772

Research Article
doi.org/10.1002/ejic.202200772

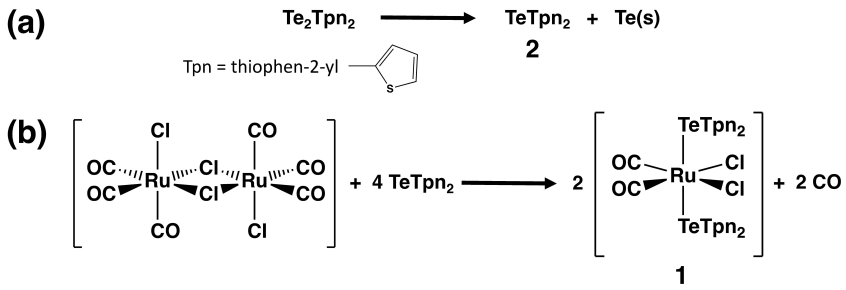

Scheme 1. (a) Decomposition of Te_2Tpn_2. (b) Ligand substitution reaction of $TeTpn_2$ with $[RuCl_2(CO)_3]_2$.

(molar ratio 1:8). The ^{125}Te NMR spectra of the three reaction mixtures are shown in Figure 1.

Whereas only one ^{125}Te NMR resonance was observed in reaction solution resulting from the initial molar ratios 1:1 [Figure 1(a)], those from 1:4 and 1:8 of the reactants, indicated the presence of two and three components, respectively [Figures 1(b) and 1(c)]. The evaporation of these solutions yielded a set of two different crystals: Those of $[RuCl_2(CO)_2(TeTpn_2)_2]$ (**1**) and a crop of crystals, which could be identified as $TeTpn_2$ (**2**) based on their isolation under the microscope and determining their crystal structure (see below). Upon dissolving the crystals of **2** in $CDCl_3$, one resonance at 402 ppm was observed in the ^{125}Te and four ^{13}C resonances were observed at 140.7, 134.0, 128.3, and 102.8 ppm. The resonance at 440 ppm is known for Te_2Tpn_2.[14]

Crystal Structures of $[RuCl_2(CO)_2(TeTpn_2)_2]$ (1) and $TeTpn_2$ (2)

The molecular structure of $[RuCl_2(CO)_2(TeTpn_2)_2]$ (**1**) with the numbering of the atoms is shown in Figure 2. The thiophen-2-yl groups turned out to be slightly disordered with the ring assuming two main orientations, which have been indicated by the letters **A** and **B** in the atom labels. The site occupation factors of the **A** rings are 0.824(13), 0.871(16), 0.940(11), and 0.775(14) for C11A-S11A, C15A-S12A, C21A-S21A, and C25A-S22A, respectively.

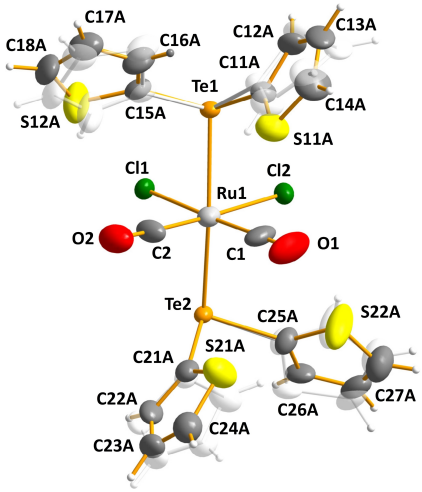

Figure 2. Molecular structure of *cct*-$[RuCl_2(CO)_2(TeTpn_2)_2]$ (**1**) indicating the numbering of the atoms. The anisotropic displacement factors are given at 50% probability level. Only the more common **A** rings of the disordered thiophen-2-yl groups have been labelled. The alternative **B** rings are shown in semi-transparent white. Selected bond parameters: Ru1-Te1 2.6496(15) Å, Ru1-Te2 2.6549(15) Å, Ru1-Cl1 2.437(3) Å, Ru1-Cl2 2.423(3) Å, Ru1-C1 1.885(14) Å, Ru1-C2 1.848(13) Å, C1-O1 1.115(15) Å, C2-O2 1.138(14) Å, Te1-Ru1-Te2 162.48(5)°, Te1-Ru1-Cl1 80.00(9)°, Te1-Ru1-Cl2 80.80(9)°, Te2-Ru1-Cl1 85.41(9)°, Te2-Ru1-Cl2 89.55(9)°, Te1-Ru1-C1 96.8(4)°, Te1-Ru1-C2 95.6(4)°, Te2-Ru1-C1 95.6(4)°, Te2-Ru1-C2 92.8(4)°.

$[RuCl_2(CO)_2(TeTpn_2)_2]$ (**1**) shows *cis*(Cl)-*cis*(CO)-*trans*($TeTpn_2$) (*cct*) conformation, as has been deduced previously for the

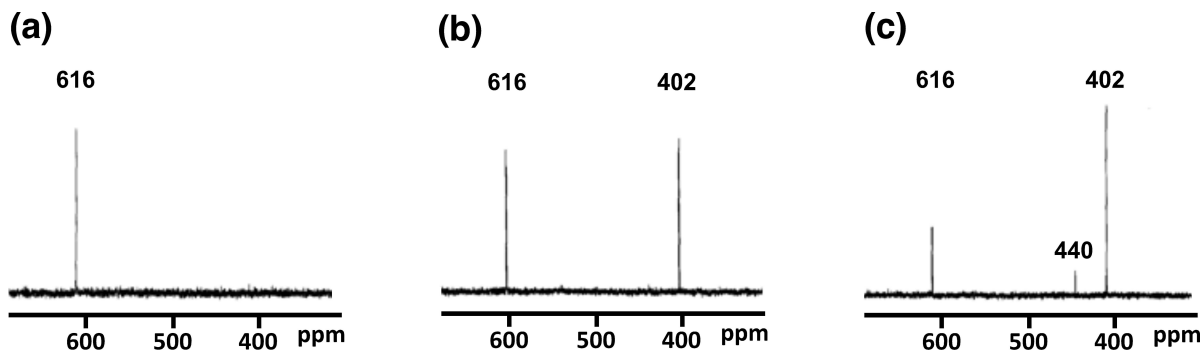

Figure 1. ^{125}Te NMR spectra of the filtered CH_2Cl_2 reaction solutions between $[RuCl_2(CO)_3]_2$ and Te_2Tpn_2 as a function of the molar ratio of the reactants. (a) Excess of $[RuCl_2(CO)_3]_2$ (molar ratio 1:1). (b) Formally stoichiometric reaction (molar ratio 1:4). (c) Excess of Te_2Tpn_2 (molar ratio 1:8). See Scheme 1.

Research Article
doi.org/10.1002/ejic.202200772

related chalcogenoether complexes.[8–13] The Ru–Te bond lengths of 2.6496(15) and 2.6549(15) Å are in good agreement with those of $[RuCl_2(CO)_2(TePh_2)_2]\cdot{}^1/_2C_6H_6$ [2.6478(7) and 2.6637(7) Å] [11] and are also consistent with all other related Ru–Te complexes.[12,15–22] All other bond parameters are also quite normal.

The crystal structure of **2** has been determined previously,[23] but it turned out that the crystals obtained by us were a different polymorph of the compound reported earlier. We therefore also determined its crystal structure.

The structure of the $TeTpn_2$ (**2**) molecule together with the labelling of the atoms and the selected bond parameters is shown in Figure 1S of Supporting Information. The asymmetric unit is composed of two half-molecules, which are both completed by symmetry. One thiophen-2-yl ring is again disordered. The more abundant **A** ring has the site occupancy factor of 0.640(11). The second thiophen-2-yl ring does not appear to be disordered. All bond parameters are quite normal, as exemplified by the Te–C bonds of 2.101(6) and 2.104(6) Å (see Figure 1S) (c.f. 2.08(1)–2.10(1) Å in the other polymorph[23]).

The solid-state lattices of the two polymorphs differ significantly. Whereas the known polymorph shows a center of symmetry in the lattice and a secondary bonding interaction of 4.0659(18) Å between the tellurium atoms of the neighbouring molecules,[23] the lattice of the current polymorph **2** shows neither the center of symmetry nor secondary tellurium-tellurium bonds. By contrast, there are aromatic ring π-σ(Te–C)* interactions between the neighbouring molecules of 3.6697(1) and 3.6817(1) Å (see the comparison of the crystal lattices of the two polymorphs in Figure 3).

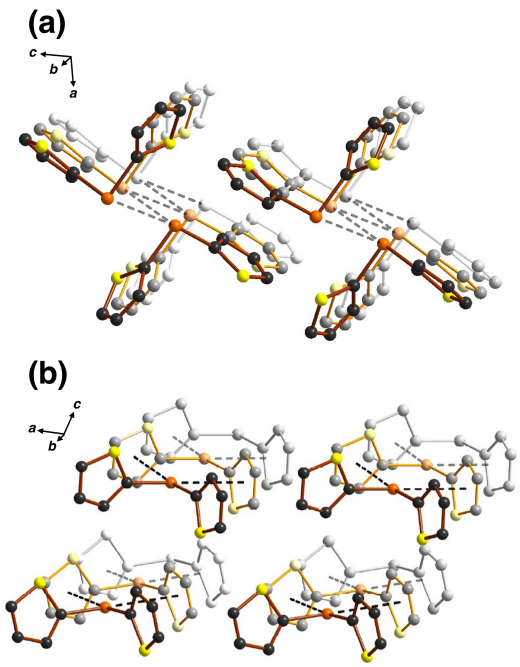

Figure 3. Packing of molecules in the two polymorphs of $TeTpn_2$ (Tpn = thiophen-2-yl, C_4H_3S). (a) Space group $P2_1/c$.[23] (b) Space group $C2$ (this work), only the more abundant component of the disordered thiophen-2-yl groups is shown for clarity.

Reaction Pathway

In order to gain an understanding of the reaction leading to the decomposition of Te_2Tpn_2, we have explored the reaction at different molar ratios by involving both the deficiency and excess of bis(thiophen-2-yl) ditelluride. It can be seen from the ^{125}Te NMR spectrum that with a significant excess of $[RuCl_2(CO)_3]_2$ [molar ratio 1:1, see Figure 1(a)], Te_2Tpn_2 has completely disappeared from the reaction solution after the reflux of 24 h, as inferred by the absence of a resonance at 440 ppm,[14] and the NMR spectrum indicates only the presence of $[RuCl_2(CO)_2(TeTpn_2)_2]$ (**1**) in the solution. The formation of a black precipitate was also observed. The yield based on limiting reagent Te_2Tpn_2 was virtually quantitative upon isolation of **1** from this solution. In the case of formal stoichiometric reaction (molar ratio 1:4) no resonance due to Te_2Tpn_2 was still observed in the final reaction solution [Figure 1(b)]. Instead, a new resonance at 402 ppm appeared in the spectrum, which was assigned to $TeTpn_2$ (**2**). With two-fold excess of Te_2Tpn_2 with respect to $[RuCl_2(CO)_3]_2$, the resonance at 402 ppm was the strongest signal in the spectrum, and it was only in this case that the weak ^{125}Te NMR resonance at 440 ppm due to undecomposed Te_2Tpn_2 was detected (*c.f.* Ref. [14]).

The compositions of the different reaction solutions could be estimated from the intensities of the ^{125}Te NMR spectra shown in Figure 1 (see Table 2S in Supporting Information). The concentrations of the products in the reaction mixtures were calculated from the initial concentrations of the reactants. They enabled the semi-quantitative estimation of the conversion of $[RuCl_2(CO)_3]_2$ during the reactions, as also shown in Table 2S.

While the 1:1 reaction is virtually complete with respect to Te_2Tpn_2, the conversion of $[RuCl_2(CO)_3]_2$ is expectedly only ca. 25%. In case of the nominally stoichiometric reaction of Te_2Tpn_2 and $[RuCl_2(CO)_3]_2$, the conversion increased to approximately 50%, and to 60% in the case of a significant excess of Te_2Tpn_2 (initial molar ratio 1:8).

The catalytic cycle leading to the decomposition of Te_2Tpn_2 that fits these observations can be proposed and is shown in Scheme 2. The PBE0-D3/def2-TZVP calculations show that this cycle is exergonic at 298 K rendering the cycle sustainable. The main driving force in the reaction appears to be the precipitation of elemental tellurium.

The energy profile and the structures of the transition states in reaction steps **I–V** are shown in Figure 4. The PBE0-D3/def2-TZVP activation energies are sufficiently small in each step. The highest individual activation energy of 55.8 kJ mol^{-1} is computed between the intermediates **I2** and **I3** for the concurrent breaking of Te–Te and formation of Te-Tpn bonds. **TSC** is the highest-energy transition state lying 66.7 kJ mol^{-1} above the total energy of the reactants $[RuCl_2(CO)_3]_2$ and Te_2Tpn_2. This reaction cycle can therefore be expected to take place slowly upon prolonged reflux in CH_2Cl_2. The activation energy of step **I** (transition state **TSA**) from the starting material to the intermediate **I1** (38.1 kJ mol^{-1}) agrees closely to that in the related ligand substitution of $[RuCl_2(CO)_3]_2$ and EMe_2 (E = S, Se, Te), the computed value of which is 35.8 kJ mol^{-1} for each chalcogenoether.[8]

Research Article
doi.org/10.1002/ejic.202200772

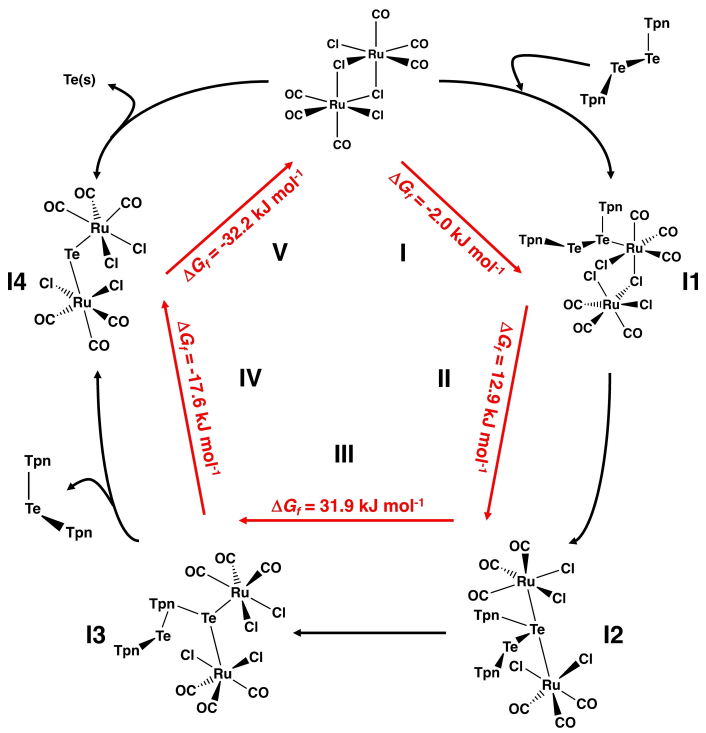

Scheme 2. The proposed catalytic cycle for the decomposition of Te_2Tpn_2 (Tpn = thiophen-2-yl, C_4H_3S) to $TeTpn_2$ (**2**) and Te(s) in dichloromethane. The energies have been computed at PBE0-D3/def2-TZVP level of theory and refer to the decomposition of $^1/_2$ moles of $[RuCl_2(CO)_3]_2$ that corresponds to the formation of one mole of *cct*-$[RuCl_2(CO)_2(TeTpn_2)_2]$ (**1**), *c.f.* Scheme 1(b). For the coordinates of all optimized species, see Table 4S.

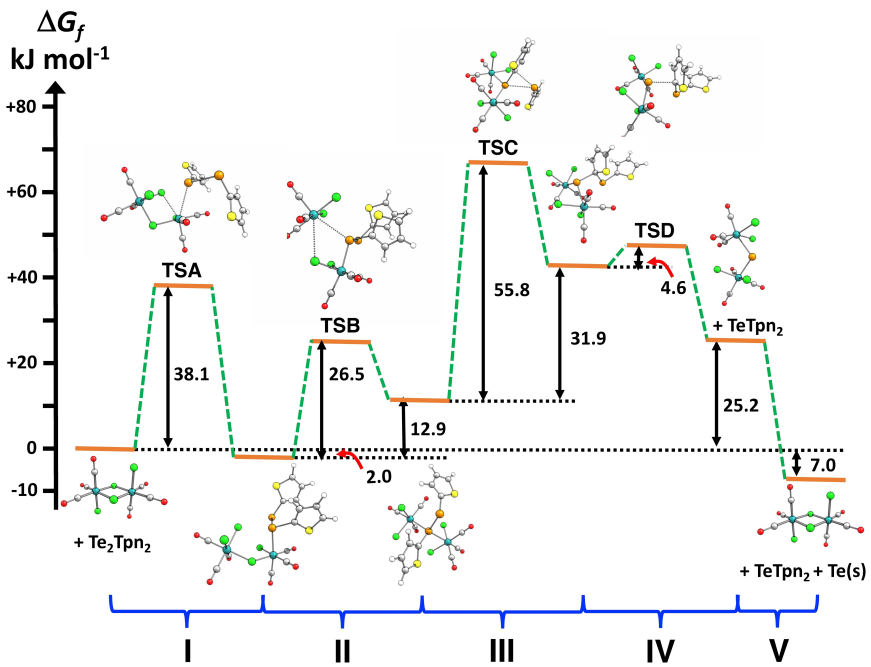

Figure 4. Energy profile of the catalytic cycle of the decomposition of Te_2Tpn_2 to $TeTpn_2$ and Te(s). The energies have been computed at PBE0-D3/def2-TZVP level of theory and refer to the decomposition of $^1/_2$ moles of $[RuCl_2(CO)_3]_2$ that corresponds to the formation of one mole of *cct*-$[RuCl_2(CO)_2(TeTpn_2)_2]$ (**1**), *c.f.* Scheme 1(b). For the coordinates of all optimized species, see Table 4S.

We have also considered other pathways for the $[RuCl_2(CO)_3]_2$-assisted cycle leading to the dissociation of Te_2Tpn_2. All alternative pathways turned out to be less favourable than the route shown in Scheme 2 and Figure 4. This is exemplified by two alternative catalytic cycles in Scheme 3.

Research Article
doi.org/10.1002/ejic.202200772

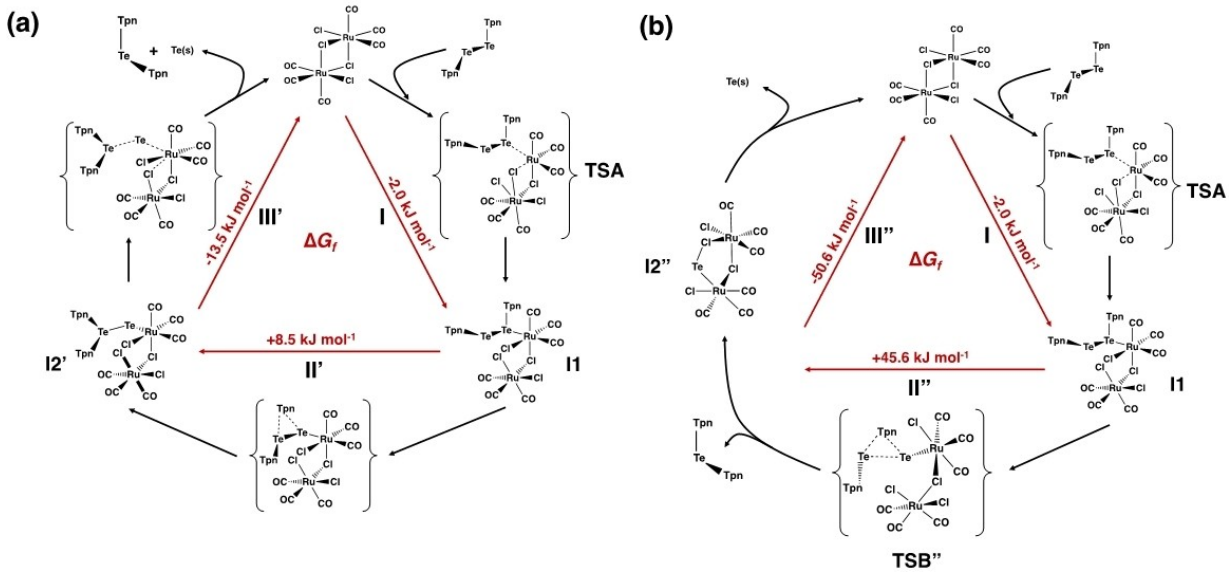

Scheme 3. Two alternative pathways for the catalytic decomposition of Te_2Tpn_2. The routes in (a) and (b) have been discussed in the text. For the coordinates of all optimized species, see Table 4S.

The cycle shown in Scheme 3(a) superficially looks a promising candidate. All Gibbs energy changes are small. The step **I** is the same as in Figure 4 with the PBE0-D3/def2-TZVP activation energy of 38.1 kJ mol^{-1}. The step **II'** involves the isomerization of the coordinated Te_2Tpn_2 to $TeTeTpn_2$ followed by the step **III'** involving decoordination and decomposition of the ligand to $TeTpn_2$ and Te(s). Whereas R_2TeTe (R = aryl group) species are not known, the relative energies of isomerization of X_2TeTe to XTeTeX (X = halogen atom) have been computed.[24] The XTeTeX isomer was generally found to be more stable than the X_2TeTe isomer. The latter, however, was stabilized with increasing electronegativity of the halogen atom. In fact, F_2TeTe was found to be slightly more stable than FTeTeF. In case of the related disulfide isomers, both F_2SS and FSSF have been isolated and structurally characterized.[25] The main problem in this reaction route is the high activation energy of the step **II'**. We have been unable to find any isomerization barrier below 100 kJ mol^{-1}. This value is consistent with the barriers calculated for the isomerization of FSSF to F_2SS.[26]

Whereas the step **I** leading to **I1** in the cycle shown in Scheme 3(b) is again the same as in other routes considered in this contribution [Schemes 2 and 3(a)], the Gibbs energy change and the activation energy in step **II"** are rather unfavorable (43.6 and 88.7 kJ mol^{-1} respectively; see Figure 2S in Supporting Information). By contrast to the pathway in Scheme 3(a), the transition state **TSB"** does not lead to the formation of the coordinated $TeTeTpn_2$ isomer but to dissociation of $TeTpn_2$ from the complex and virtually barrierless formation of the five-membered ring intermediate **I2"**. While we have not attempted to find a transition state for the last step **III"** in Scheme 3(b), the relatively large Gibbs energy change during this step and the formation of solid tellurium are expected to provide the driving force for the reaction.

Once $TeTpn_2$ has been formed, the reaction pathway for the ligand substitution in $[RuCl_2(CO)_3]_2$ expectedly follows the same route with similar energetics, as has previously been computed for the related reactions of ERR' (E = S, Se, Te; R, R' = Me, Ph).[8] This is shown in Scheme 4.

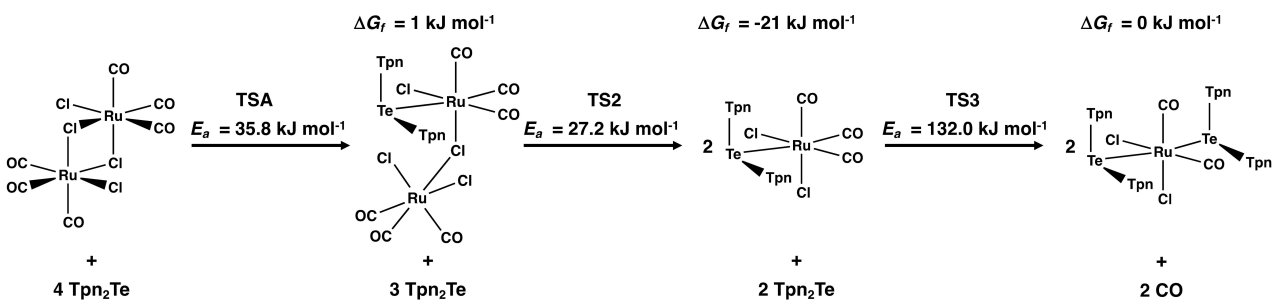

Scheme 4. The PBE0-D3/def2-TZVP Gibbs energies and activation energies for the ligand substitution of $TeTpn_2$ in $[RuCl_2(CO)_3]_2$ in dichloromethane. The energy values are scaled for the formation of one mole of *cct*-$[RuCl_2(CO)_2(TeTpn_2)_2]$ (**1**), *c.f.* Scheme 1(b). For the coordinates of all optimized species, see Table 4S.

Research Article
doi.org/10.1002/ejic.202200772

It is interesting to note that the PBE0-D3/def2-TZVP Gibbs energy change in the final substitution step is 0 kJ mol^{-1}. That of the corresponding step computed at the same level of theory involving $TeMe_2$, TeMePh, and $TePh_2$ are −15.7, −12.5, and −7.9 kJ mol^{-1}, respectively.[8] While these values have been computed in THF, we have previously shown that the energetics are virtually independent of the solvent. The current value of 0 kJ mol^{-1} follows the trend that the Gibbs energy change becomes less favourable with increasing electron-withdrawing power of the organic substituent of the telluride. While the final step is energy neutral, the driving force for the formation of the final complex is the leaving of gaseous carbon monoxide from the equilibrium mixture.

The energetics shown in Schemes 2 and 4, and Figure 4 indicate that the decomposition of Te_2Tpn_2 to $TeTpn_2$ is somewhat faster than the ligand substitution leading to the final product *cct*-$[RuCl_2(CO)_2(TeTpn_2)_2]$ (**1**). This has also been verified experimentally. The stoichiometric reaction was carried out in the absence of light by stirring the reactants in CH_2Cl_2 and monitoring the composition of the solution using ^{125}Te NMR spectroscopy (see Figure 3S in Supporting Information). After one day, the ^{125}Te NMR spectrum of the reaction solution showed the major resonance of unreacted Te_2Tpn_2 (440 ppm), but a minor resonance of $TeTpn_2$ at 402 ppm could also be observed [see Figure 2S(a) in Supporting Information]. After seven days, the resonance due to $TeTpn_2$ showed the highest intensity and Te_2Tpn_2 was seen as a minor component in the solution [see Figure 2S(b) in Supporting Information]. The intensity of the resonance of the complex **1** increased only slowly.

We have also carried out two control reactions. The first involved the prolonged exposure of the Te_2Tpn_2 solution in sunlight, during the course of which the precipitation of elemental tellurium took slowly place, and the ^{125}Te NMR spectrum of the solution indicated the presence of both Te_2Tpn_2 and $TeTpn_2$. Analogous photochemical decomposition has been observed for $Te_2(CH_2Ph)_2$.[27] The decomposition of $Te_2(CH_2Ph)_2$ was also found to take place thermally in 10 min at 120 °C under red light in nitrogen.

The second control experiment involved the reflux of the CH_2Cl_2 solution of Te_2Tpn_2 for several hours without $[RuCl_2(CO)_3]_2$ in the absence of light. No decomposition of the ditelluride was observed. It can therefore be concluded that the decomposition of Te_2Tpn_2 is assisted by $[RuCl_2(CO)_3]_2$. Reminiscent of the present findings, diaryl tellurides TeR_2 have been prepared utilizing the catalytic decomposition of Te_2R_2 involving copper catalysts.[28–30] While no mechanism has been suggested for these transformations, it is possible that they proceed in a similar manner as shown in this contribution.

Conclusions

The reflux of the CH_2Cl_2 solution of $[RuCl_2(CO)_3]_2$ and Te_2Tpn_2 (Tpn = thiophen-2-yl, C_4H_3S) in the absence of light resulted in the decomposition of the ditelluride to $TeTpn_2$ and elemental tellurium followed by the formation of *cct*-$[RuCl_2(CO)_2(TeTpn_2)_2]$ [*cct* = *cis*(Cl)-*cis*(CO)-*trans*-$(TeTpn_2)$]. The reaction was monitored by ^{125}Te NMR spectroscopy, and a pathway has been proposed by PBE0-D3/def-TZVP calculations. The plausible route involves the $[RuCl_2(CO)_3]_2$-catalyzed decomposition of Te_2Tpn_2 to $TeTpn_2$ and Te(s). The catalytic cycle is exergonic with the precipitation of elemental tellurium as the driving force. Once $TeTpn_2$ is formed, it reacts with $[RuCl_2(CO)_3]_2$ to afford *cct*-$[RuCl_2(CO)_2(TeTpn_2)_2]$. The energetics and kinetics of the last part of the reaction are very similar to the related ligand substitution reaction involving ERR′ (E = S, Se, Te; R, R′ = Me, Ph).[8]

Experimental Section

Materials: All reactions and manipulations of air- and moisture-sensitive compounds were carried out in the absence of light under an inert atmosphere by using Schlenk techniques. Bis(thiophen-2-yl) ditelluride was prepared according to the literature procedure.[31] Dichloromethane (Lab-Scan) was distilled over CaH_2 and purged with argon before use. $[RuCl_2(CO)_3]_2$ (Johnson Matthey) was used as purchased.

NMR spectroscopy: The ^{1}H, ^{13}C{^{1}H}, and ^{125}Te spectra were recorded on a Bruker DPX 400 spectrometer operating at 400.00, 100.61, and 126.24 MHz, respectively. The ^{13}C and ^{125}Te spectral widths were 24.038 and 75.758 kHz, respectively, the ^{13}C and ^{125}Te pulse widths were 4.0 and 10.0 μs, respectively and the pulse delay was 4.0 s in both cases. Tetramethylsilane and a saturated D_2O solution of H_6TeO_6 were used as internal and external standards, respectively. The ^{1}H and ^{13}C chemical shifts are reported relative to the standard, and the ^{125}Te chemical shifts relative to neat Me_2Te {$\delta(Me_2Te) = \delta(H_6TeO_6) + 710.9$[32]}.

X-ray diffraction: Diffraction data for $[RuCl_2(CO)_2(TeTpn_2)_2]$ and $TeTpn_2$ were collected at 120 K on a Nonius Kappa CCD diffractometer using graphite monochromated Mo Kα radiation (λ = 0.71073 Å). Crystal data and the details of the structure determinations are presented in Table 1S in Supporting Information. The structures were solved by direct methods using SHELXS-2016 and refined using SHELXL-2016.[33,34] After the full-matrix least-squares refinement of the non-hydrogen atoms with anisotropic thermal parameters, the hydrogen atoms were placed in calculated positions. In the final refinement, the calculated hydrogen atoms were riding with the carbon atom they were bonded to. The isotropic thermal parameters of the aromatic hydrogen atoms were fixed at 1.2 to that of the corresponding carbon atom. The scattering factors for the neutral atoms were those incorporated with the program.

Reaction of Te_2Tpn_2 with $[RuCl_2(CO)_3]_2$: A series of three reactions was carried out by adding Te_2Tpn_2 to a suspension of $[RuCl_2(CO)_3]_2$ in CH_2Cl_2 (10 mL): (1) an excess of $[RuCl_2(CO)_3]$, (2) formally stoichiometric molar amounts (see Scheme 1), (3) an excess of Te_2Tpn_2. The reaction mixture was refluxed for 24 h to give an orange solution with black precipitation. The solution was filtered and the solvent was evaporated affording generally a mixture of orange and colourless crystals. In case of the reaction using equimolar amounts of the reactants, only one crop of orange crystals was obtained at this stage. They were dried in vacuum and identified as $[RuCl_2(CO)_2(TeTpn_2)_2]$. Crystals suitable for X-ray crystallography were grown from a CH_2Cl_2 solution at +3 °C. Anal. calcd. for $C_{18}H_{16}Cl_2O_2RuS_4Te_2$: C, 25.88; H, 1.53; S 14.76. Found: C, 26.50; H, 1.48; S 15.72. NMR (δ, ppm) ($CDCl_3$): ^{1}H 7.67 (dd, *J* 3.4 and 3.8 Hz), 7.52 (dd, *J* 3.4 and 4.7 Hz), 7.12 (dd, *J* 3.8 and 4.7 Hz), ^{13}C 106.5, 128.8, 134.6, 138.9, 191.4 (CO); ^{125}Te 616. The molar amounts and the semi-quantitative product distributions in the reactions have been given in Table 2S and the 1H and ^{13}C{^{1}H} NMR spectra in Figure 2S in Supporting Information.

Computational Details: Structures were optimized using Gaussian 16 program package,[35] PBE0 DFT hybrid functional [36–38], def2-TZVP basis sets,[39,40] and Grimme's empirical model with Becke-Johnson damping (D3) to treat the dispersion forces.[41–43] Structures in dichloromethane solutions were optimized using implicit C-PCM solvent model[44,45] to describe the solvent effects. Formation of Te(s) in one of the reactions was accounted by modelling Te_2(g) and taking the literature values for the formation of Te_2(g) [$2Te(s) \leftrightarrow Te_2(g)$ $\Delta H = +168.2\ kJ\,mol^{-1}$ and $\Delta G(298\ K) = +118.0\ kJ\,mol^{-1}$].[46] The total energies and optimized geometries of all species computed in this work are shown in Supporting Information (Tables 3S and 4S, respectively).

Supporting Information: Crystal data of **1** and **2**, molecular structure of $TeTpn_2$, composition of reaction mixtures, DFT energetics and optimized geometries, some further details of the reaction pathway.

Deposition Numbers 2060504 (for **1**) and 2060503 (for **2**) contain the Supporting crystallographic data for this paper. These data are provided free of charge by the joint Cambridge Crystallographic Data Centre and Fachinformationszentrum Karlsruhe Access Structures service.

Acknowledgements

The Alfred Kordelin Foundation (Grant no. 210317) and Tauno Tönning Research Foundation (M. T.), and provision of computational resources by Prof. Heikki Tuononen (University of Jyväskylä) (J. M. R.) are gratefully acknowledged.

Conflict of Interest

The authors declare no conflict of interest.

Data Availability Statement

The data that support the findings of this study are available in the supplementary material of this article.

Keywords: bis(thiophen-2-yl) ditellane · reaction mechanisms · ruthenium · tellurium · X-ray diffraction

[1] S. G. Murray, F. R. Hartley, *Chem. Rev.* **1981**, *81*, 365–414.
[2] H. J. Gysling, *Coord. Chem. Rev.* **1982**, *42*, 133–244.
[3] E. G. Hope, W. Levason, *Coord. Chem. Rev.* **1993**, *122*, 109–170.
[4] W. Levason, S. D. Orchard, G. Reid, *Coord. Chem. Rev.* **2002**, *225*, 159–199.
[5] A. K. Singh, P. K. Raghavendra, G. Singh, S. Bali, *Phosphor. Sulfur Silicon Relat. Elem.* **2005**, *180*, 903–170.
[6] V. K. Jain, R. S. Chauhan, *Coord. Chem. Rev.* **2016**, *306*, 270–301.
[7] R. S. Chauhan, N. Shivran, *RSC Adv.* **2017**, *7*, 55175–55198.
[8] M. Taimisto, T. Bajorek, J. M. Rautiainen, T. A. Pakkanen, R. Oilunkaniemi, R. S. Laitinen, *Dalton Trans.* **2022**, *51*, 11747–11757.
[9] W. Hieber, P. John, *Chem. Ber.* **1970**, *103*, 2161–2177.
[10] P. John, *Chem. Ber.* **1970**, *103*, 2178–2196.
[11] R. Oilunkaniemi, R. S. Laitinen, M. Ahlgrén, *Inorg. Chem. Commun.* **2000**, *3*, 8–10.
[12] M. Taimisto, T. Bajorek, R. Oilunkaniemi, R. S. Laitinen, M. Ahlgrén, *Z. Naturforsch B: J. Chem. Sci.* **2003**, *58*, 959–964.
[13] L. Vigo, M. J. Poropudas, R. Oilunkaniemi, R. S. Laitinen, *J. Organomet. Chem.* **2008**, *693*, 557–561.
[14] R. Oilunkaniemi, R. S. Laitinen, M. Ahlgrén, *Z. Naturforsch. B* **2000**, *55*, 1–8.
[15] W. Levason, G. Reid, V.-A. Tolhurst, *J. Chem. Soc. Dalton Trans.* **1998**, 3411–3416.
[16] W. Levason, S. D. Orchard, G. Reid, *Chem. Commun.* **1999**, 1071–1072.
[17] W. Levason, S. D. Orchard, G. Reid, V.-A. Tolhurst, *J. Chem. Soc. Dalton Trans.* **1999**, 2071–2076.
[18] W. Levason, S. D. Orchard, G. Reid, *J. Chem. Soc. Dalton Trans.* **2000**, 4550–4554.
[19] W. Levason, S. D. Orchard, G. Reid, *Inorg. Chem.* **2000**, *39*, 3853–3859.
[20] W. Levason, B. Patel, G. Reid, A. J. Ward, *J. Organomet. Chem.* **2001**, *619*, 218–225.
[21] W. Levason, M. Nirwan, R. Ratnani, G. Reid, N. Tsoureas, M. Webster, *Dalton Trans.* **2007**, 439–448.
[22] W. Levason, L. P. Ollivere, G. Reid, M. Webster, *J. Organomet. Chem.* **2010**, *695*, 1346–1352.
[23] G. Bandoli, J. Bergman, K. J. Irgolic, A. Grassi, G. C. Pappalardo, *Z. Naturforsch. B* **1985**, *40*, 1157–1160; A. K. S. Chauhan, P. Singh, R. C. Srivastava, R. J. Butcher, *CSD Commun. (Private Communication)* **2016**, CCDC 802240.
[24] M. El-Hamdi, J. Poater, F. M. Bickelhaupt, M. Sola, *Inorg. Chem.* **2013**, *52*, 2458–2465.
[25] F. Seel, *Adv. Inorg. Chem. Radiochem.* **1974**, *16*, 297–333, and references therein.
[26] Y. Zeng, L. Meng, X. Li, S. Zheng, *J. Phys. Chem.* **2007**, *111*, 9093–9101.
[27] H. K. Spencer, M. P. Cava, *J. Org. Chem.* **1977**, *42*, 2937–2939.
[28] R. Weiss, E. Aubert, P. Pale, Y. Mamane, *Angew. Chem. Int. Ed.* **2021**, *35*, 19281–19286.
[29] M. Oba, Y. Okada, M. Endo, K. Tanaka, K. Nishiyama, S. Shimada, W. Ando, *Inorg. Chem.* **2010**, *49*, 10680–10686.
[30] Y. Okada, M. Oba, A. Arai, K Tanaka, K. Nishiyama, W. Ando, *Inorg. Chem.* **2010**, *49*, 383–385.
[31] L. Engman, M. P. Cava, *Organometallics* **1982**, *1*, 470–473.
[32] M. J. Collins, G. J. Schrobilgen, *Inorg. Chem.* **1985**, *24*, 2608–2614.
[33] G. M. Sheldrick, *Acta Crystallogr. Sect. A* **2008**, *64*, 112–122.
[34] G. M. Sheldrick, *Acta Crystallogr. Sect. A* **2015**, *71*, 3–8.
[35] M. J. Frisch, G. W. Trucks, H. B. Schlegel, G. E. Scuseria, M. A. Robb, J. R. Cheeseman, G. Scalmani, V. Barone, G. A. Petersson, H. Nakatsuji, X. Li, M. Caricato, A. V. Marenich, J. Bloino, B. G. Janesko, R. Gomperts, B. Mennucci, H. P. Hratchian, J. V. Ortiz, A. F. Izmaylov, J. L. Sonnenberg, D. Williams-Young, F. Ding, F. Lipparini, F. Egidi, J. Goings, B. Peng, A. Petrone, T. Henderson, D. Ranasinghe, V. G. Zakrzewski, J. Gao, N. Rega, G. Zheng, W. Liang, M. Hada, M. Ehara, K. Toyota, R. Fukuda, J. Hasegawa, M. Ishida, T. Nakajima, Y. Honda, O. Kitao, H. Nakai, T. Vreven, K. Throssell, J. A. Montgomery Jr., J. E. Peralta, F. Ogliaro, M. J. Bearpark, J. J. Heyd, E. N. Brothers, K. N. Kudin, V. N. Staroverov, T. A. Keith, R. Kobayashi, J. Normand, K. Raghavachari, A. P. Rendell, J. C. Burant, S. S. Iyengar, J. Tomasi, M. Cossi, J. M. Millam, M. Klene, C. Adamo, R. Cammi, J. W. Ochterski, R. L. Martin, R. L.; K. Morokuma, O. Farkas, J. B. Foresman, D. J. Fox, Gaussian 16, Rev. C.01, Gaussian, Inc.: **2016**.
[36] J. P. Perdew, K. Burke, M. Ernzerhof, *Phys. Rev. Lett.* **1996**, *77*, 3865–3868; *Phys. Rev. Lett.* **1997**, *78*, 1396.
[37] J. P. Perdew, M. Ernzerhof, K. Burke, *J. Chem. Phys.* **1996**, *105*, 9982–9985.
[38] C. Adamo, V. Barone, *J. Chem. Phys.* **1999**, *110*, 6158–6170.
[39] F. Weigend, M. Haser, H. Patzelt, R. Ahlrichs, *Chem. Phys. Lett.* **1998**, *294*, 143–152.
[40] F. Weigend, R. Ahlrichs, *Phys. Chem. Chem. Phys.* **2005**, *7*, 3297–3305.
[41] S. Grimme, J. Antony, S. Ehrlich, H. Krieg, *J. Chem. Phys.* **2010**, *132*, 154104/1-154104/19.
[42] L. A. Burns, A. Vazquez-Mayagoitia, B. G. Sumpter, C. D. Sherrill, *J. Chem. Phys.* **2011**, *134*, 084107/1-084107/25.
[43] S. Grimme, S. Ehrlich, L. Goerigk, *J. Comput. Chem.* **2011**, *32*, 1456–1465.
[44] V. Barone, M. Cossi, *J. Phys. Chem. A* **1998**, *102*, 1995–2001.
[45] M. Cossi, N. Rega, G. Scalmani, V. Barone, *J. Comb. Chem.* **2003**, *24*, 669–681.
[46] W. M. Haynes (Ed.), *CRC Handbook of Chemistry and Physics*, 96th Ed., CRC Press, Taylor and Francis: Boca Raton, **2016**.

Manuscript received: December 16, 2022
Revised manuscript received: February 18, 2023
Accepted manuscript online: February 20, 2023